Jpn. J. Appl. Phys. Vol. 41 (2002) pp. L 1016–L 1018
Part 2, No. 9A/B, 15 September 2002

Simple X-Ray Dark- and Bright-Field Imaging Using Achromatic Laue Optics

Masami ANDO[1,2,*], Anton MAKSIMENKO[2], Hiroshi SUGIYAMA[1,2], Wanwisa PATTANASIRIWISAWA[2], Kazuyuki HYODO[1,3] and Chikao UYAMA[4]

[1]*Photon Factory, Institute of Materials Structure Science, High Energy Accelerator Research Organization (KEK), 1-1 Oho, Tsukuba, Ibaraki 305-0801, Japan*
[2]*Department of Photo-Science, School of Advanced Studies, Graduate University for Advanced Studies (GUAS), Shonan International Village, Hayama, Miura, Kanagawa 240-0193, Japan*
[3]*Department of Material Structure Science, School of Physical Mathematics, Graduate University for Advanced Studies (GUAS), 1-1 Oho, Tsukuba, Ibaraki 305-0801, Japan*
[4]*Department of Clinical Engineering, Faculty of Health Sciences, Hiroshima International University, Kurose-chou, Kamo-gun, Hiroshima 724-0695, Japan*

(Received March 4, 2002; accepted for publication July 9, 2002)

X-ray dark-field and bright-field imaging in the Laue geometry has been successfully demonstrated. Using a Bragg-case asymmetric monochromator that produces an X-ray beam with a 0.3 μrad divergence incident onto an object and a Laue geometry analyzer that can simultaneously provide dark-field imaging (DFI) and bright-field imaging (BFI). The DFI has only an X-ray refraction component on the object without illumination, while the BFI has reasonable illumination. This was achieved by a 1.075 mm thick silicon analyzer with 4, 4, 0 diffraction at 35 keV X-ray photon energy. An image of an insect embedded in polymethylmethacrylate, which can not be visualized by absorption, has been obtained. [DOI: 10.1143/JJAP.41.L1016]

KEYWORDS: X-ray dark-field imaging, X-ray bright-field imaging, asymmetric monochromator, analyzer, refraction contrast, synchrotron radiation, silicon

A new idea concerning very simple X-ray dark-field and bright-field imaging in Laue geometry that has never been proposed before is presented here. Since 1989, various refraction-based imaging[1–15] techniques have been proposed. All of these have originated from X-ray shadow micrography pioneered by Cosslett and Nixon in 1951.[16,17] This may correspond to imaging in the visible-light region, as described in the literature by Born and Wolf.[18] These techniques involve a neutron imaging system using a Bragg diffraction analyzer,[1–4] and X-ray imaging systems without an analyzer,[5,15] with Laue analyzer,[6] with a Bragg analyzer[7,8,12–14] and with no optics.[9–11] All of these techniques, in principle, might be categorized as bright-field imaging under a special analyzer condition.[6–8,12–14] We have recently developed dark-field imaging using new X-ray Laue[19,20] and Bragg[21] optics. The dark-field imaging in Laue geometry[19,20] proposed is very advantageous over the previous imaging developed by others[1–4,6–8,12–14] because one does not have to take a series of pictures while changing the angle of the analyzer crystal; One can simply obtain clear dark- and bright-field image of an object in a single shot.

The deflection angle, $\Delta(x, y: k)$,[19–21] associated with a refraction contrast can be described as follows:

$$\Delta(x, y: k) \propto -\int_{z_0}^{z_1} \partial\delta(x, y, z: k)/\partial x dz, \qquad (1)$$

where $\delta(x, y, z: k)$ is related to the refractive index, $n = 1 - \delta(x, y, z: k)$, z is the direction of the X-ray beam, z_0 and z_1 denote the coordinates where the X-rays go into and out of the object, respectively, and let refraction take place in the (z, x) plane.

In our X-ray dark-field and bright-field imaging arrangement shown in Fig. 1, the Laue geometry of diffraction in an achromatic arrangement, where two diffracting planes involving a monochromator M and an analyzer crystal A are in a $(+, -)$ parallel arrangement, is essential so that imaging receives no effect of wavelength spread that may otherwise blur the image contrast. We have chosen the asymmetric factor b (refer to ref. 22) to be 0.05 at M so that one can provide the beam $P(W)$ with divergence of 0.3 μrad incident onto the object $Q(W)$ located between M and A. Thus $P(W)$ has been modulated into $R(W)$ due to $Q(W)$. The refraction angles for almost all boundaries of ordinary materials should be on the order of 1 μrad or greater than the angular spread of $P(W)$. This $R(W)$ will be analyzed by A that has a function of $I_O(W)$ along the direction of forward diffraction and $I_G(W)$ along the diffraction direction. $I_O(W)$ has the potential to suppress $R(W)$ completely at $|W| < 1$. Thus $D(W) = I_O(W)R(W)$ after A along the forward diffraction direction corresponds to dark-field imaging (DFI) because there is no apparent X-ray background intensity existing at $|W| < 1$ due to the structure of $I_O(W)$, while $B(W) = I_G(W)R(W)$ corresponds to bright-field imaging (BFI) along the diffraction direction because of the nature of $I_G(W)$. The beams $D(W)$ and $B(W)$ will be stored as a dark-field image and a bright-field image, respectively.

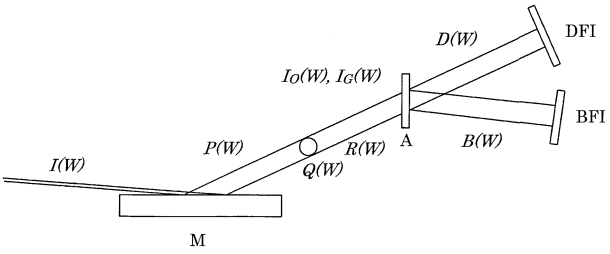

Fig. 1. X-ray optics setup for simultaneously producing dark-field image and bright-field images. The incident beam $I(W)$ is incident onto an asymmetric monochromator M that reduces outgoing beam divergence by a factor of 0.2. The beam divergence of $P(W)$, which is incident onto object $Q(W)$, has 0.3 μrad. The modulated beam $R(W)$ contains information on $Q(W)$; $R(W)$ splits into $D(W)$ and $B(W)$ due to $I_O(W)$ and $I_G(W)$, respectively. $D(W)$ and $B(W)$ lead to production of a dark-field image and a bright-field images using an imaging device, respectively.

Two reflectivity functions $I_O(W)$ and $I_G(W)$ at A can be

*E-mail address: masami.ando@kek.jp

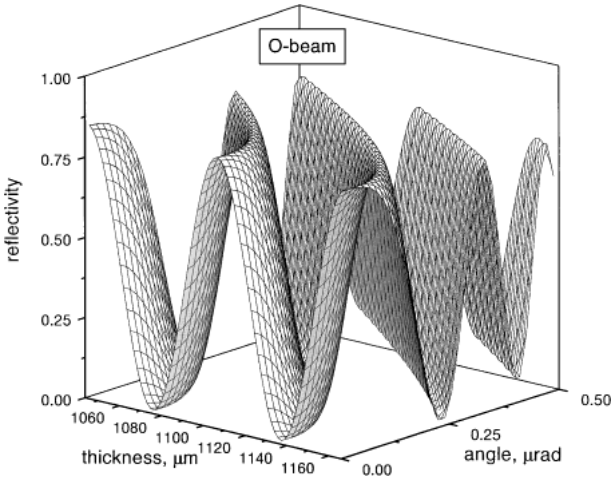

Fig. 2. Reflectivity $I_O(W)$ versus the analyzer thickness t under the experimental condition of 1.075 mm, the angular coordinate W for 4, 4, 0 reflection and the X-ray energy of 35 keV. At $|W| = 0$, $I_O(W)$ is almost zero in the case of no absorption.

expressed if the X-rays undergo no absorption as follows:

$$I_O(W) = \sin^2(t\pi\sqrt{1+W^2}/\Lambda)/(1+W^2), \quad (2)$$

$$I_G(W) = (\cos^2(t\pi\sqrt{1+W^2}/\Lambda) + W^2)/(1+W^2), \quad (3)$$

$$I_O(W) + I_G(W) = 1, \quad (4)$$

where t, W, Λ are thickness of A, deviation of the angle from the Bragg condition and the extinction distance, respectively. W can be expressed as $W = 2\Lambda \sin\theta_B(\theta - \theta_B - \Delta\theta_0)/\lambda$, where $\Lambda = \lambda\cos\theta_B/|P\|\chi_G|$ is the extinction distance, P the polarization factor, λ the X-ray wavelength, $\chi_G = -r_e\lambda^2 F_G/\pi V_C$ the polarizability, where r_e is the classical radius of electron, F_G the crystal structure form factor, V_C the volume of unit cell, θ the angle that deviated from the Bragg angle θ_B and $\Delta\theta_0$ correction of the Bragg angle due to refraction expressed as $\Delta\theta_0 = 2(1-n)/\sin^2\theta_B$. Equations (2) and (3) can be simplified as $I_O(W)|_{W=0} = \sin^2(t\pi/\Lambda)$ and $I_G(W)|_{W=0} = \cos^2(t\pi/\Lambda)$, respectively, at $W = 0$ so that $I_O(0)$ becomes 0%, while $I_G(0)$ 100% with periodicity of $t = p\Lambda$ where p is integer. Figure 2 shows $I_O(W)$ as a function of t and W under an experimental condition of $t = 1.075$ mm and the X-ray energy of 35 keV. The angular range in terms of W is shown only from 0.0 μrad to 0.50 μrad.

An explanation for dark-field and bright-field imaging is given as follows: first prepare an extremely straight forward beam $P(W)$ as shown in Fig. 3(a) using asymmetric diffraction[22] at M in Fig. 1. The horizontal axis should correspond to the angle, and the vertical axis to the power of the X-rays. Second, $P(W)$ that enters the object $Q(W)$ shown in Fig. 3(b) that has, for instance, an octahedral shaped polygon as shown in the inset between (b) and (c), may receive the refraction effect, either from the left or right or both directions, against the incident beam direction. As a result, the X-rays $R(W)$ which exit from $Q(W)$ may possess information on the object as shown in Fig. 3(c). Mathematically, $R(W)$ should be the convolution of $P(W)$ and $Q(W)$. Figure 3(d) shows the reflection profile $I_O(W)$ at A along the direction of forward diffraction. Due to this function of an angular filter apparently the central part of $R(W)$ has been suppressed as shown in Fig. 3(e) due to $I_O(W)$. This is called dark-field imaging $D(W)$. On the other hand, due to the other function $I_G(W)$, as shown in Fig. 3(f) bright-field imaging $B(W)$ is available, as shown in Fig. 3(g).

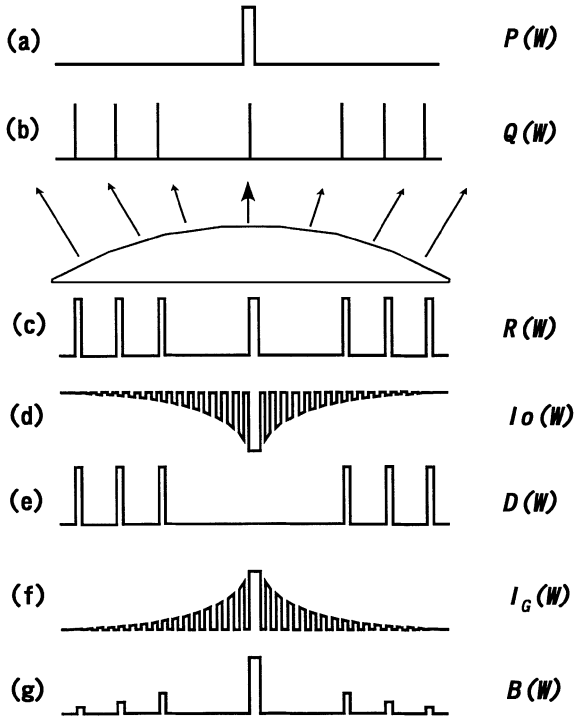

Fig. 3. Diagram showing how DFI and BFI can be formed. The horizontal axis represents the angular scale represented by W, while the vertical axis represents the power of X-rays. (a) shows an incident beam profile $P(W)$. $P(W) = 1$ for $|W| < 1$, 0 for $|W| \geq 1$, where $W = \pm 1$ corresponds to a rocking curve width for asymmetric 4, 4, 0 diffraction that has the order of 0.15 μrad; (b) represents a schematic angular distribution of object $Q(W)$ as shown in the inset between (b) and (c). This shows a model with an 8-face polygon whose refractive index is for vacuum or larger than that of its surrounding atmosphere; (c) represents the angular distribution $R(W)$ that has information on $Q(W)$ as shown in $R(W) = P(W) * Q(W)$, where $*$ represents convolution of the two functions; (d) represents a transmission function $I_O(W)$ of an analyzer crystal A along the forward diffraction direction; (e) $D(W) = I_O(W)R(W)$ the intensity profile of the beam after A along the forward diffraction direction. This corresponds to DFI because no apparent illumination light remains; (f) The transmission function $I_G(W)$ along the diffraction direction of A, (g) $B(W) = I_G(W)R(W)$ that can be BFI because an image due to refraction involves the illumination light as well.

The advantages of our method over the previous methods are as follows: first, our system is very simple. It only needs a parallel setting of two diffracting planes at M and A that should satisfy the thickness condition in eq. (1) for $I_O(W) = 0$ at $W = 0$. This can provide complete dark-field and bright-field imaging simultaneously in a single shot at $W = 0$. Also only a small distance between A and DFI or BFI is required. The contrast of all previous imaging techniques such as those by Ingal and Beliaevskaya,[6] Wilkins' group[7,8,10,12] and Chapman's group[13,14] should locate in-between dark-field imaging and bright-field imaging. Their background could not be suppressed 100% if the Bragg angle at $|W| \gg 0$ is taken.

An experiment was performed at beamline BL14B[23] using a radiation source from a 5 T vertical wiggler at the Photon Factory and at BL20B[24,25] at the 8 GeV SPring-8 storage ring. Very good agreement between calculated and experimental values of $I_O(W)$ and $I_G(W)$ has been confirmed. Images were stored on a nuclear plate which has an exposure

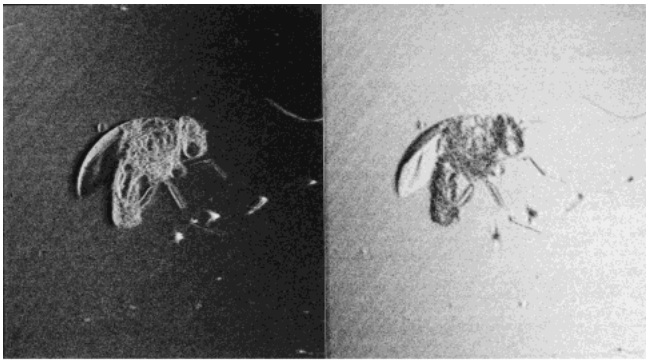

(a) (b)

Fig. 4. (a) Dark-field image and (b) bright-field images of an insect embedded in polymethylmethacrylate. The field size is 5 mm × 5 mm. Exposure time using a nuclear plate was approximately 60 s. The dark-field image (a) has an almost completely dark background.

time of approximately 60 s.

Figure 4(a) shows an image of the DFI mode of an insect embedded in polymethylmethacrylate and (b) the BFI mode. Figure 4(a) shows apparently almost no background. The field is 5 mm × 5 mm.

This work was conducted under approval of the Photon Factory Program Advisory Committee at BL14B (2001G187), the SPring-8 Program Advisory Committee at BL20B (2000B0576-CL-np, 2001B0439-NM-np) and the Hyogo Prefecture Program Advisory Board at the SPring-8 Hyogo Beamline BL24XU (C01B24XU-5054N). We thankfully acknowledge funds received from the KEK Joint Development Research 2002 and the GUAS Joint Research Project (Soken/K01-5).

1) K. M. Podurets, V. A. Somenkov and S. Sh. Shil'shtein: Zh. Tekh. Fiz. **59** (1989) 115. Translation: Sov. Phys. Tech. Phys. **34-6** (1989) 654.
2) K. M. Podurets, V. A. Somenkov and S. Sh. Shil'shtein: Physica B **156/157** (1989) 691.
3) K. M. Podurets, V. A. Somenkov, R. R. Chistyakov and S. Sh. Shil'shtein: Physica B **156/157** (1989) 694.
4) V. A. Somenkov, A. K. Tkalich and S. Sh. Shil'stein: Zh. Tech. Fiz. **61** (1991) 197. Translation: Sov. Phys. Tech. Phys. **36-11** (1991) 1309.
5) A. Snigirev, I. Snigireva, V. Kohn, S. Kuznetsov and I. Schelokov: Rev. Sci. Instrum. & Methods **66** (1995) 5486.
6) V. N. Ingal and E. A. Beliaevskaya: J. Phys. D **28** (1995) 2314.
7) T. J. Davis, D. Gao, T. E. Gureyev, A. W. Stevenson and S. W. Wilkins: Nature **373** (1995) 595.
8) T. J. Davis, T. E. Gureyev, D. Gao, A. W. Stevenson and S. W. Wilkins: Phys. Rev. Lett. **74** (1995) 3173.
9) K. A. Nugent, T. E. Gureyev, D. F. Cookson, D. Paganin and Z. Barnea: Phys. Rev. Lett. **77** (1996) 2961.
10) S. W. Wilkins, T. E. Gureyev, D. Gao, A. Pogany and A. W. Stevenson: Nature **384** (1996) 335.
11) P. Clotens, R. Barrett, J. Bruchel, J.-P. Guigay and M. Shlenker: J. Phys. D **29** (1996) 133.
12) D. Gao, T. E. Gureyev, A. Pogany, A. W. Stevenson and S. W. Wilkins: *Medical Applications of Synchrotron Radiation*, eds. M. Ando and C. Uyama (Springer-Verlag, Tokyo, 1998) p. 63.
13) D. Chapman, W. Thomlinson, F. Arfelli, N. Gmuer, Z. Zhong, R. Menk, R. E. Johnson, D. Washburn, E. Pisano and D. Sayers: Rev. Sci. Instrum. Methods **67** (1996) 3360.
14) W. Thomlinson, D. Chapman, Z. Zhong, R. E. Johnston and D. Sayers: *Medical Applications of Synchrotron Radiation*, eds. M. Ando and C. Uyama (Springer-Verlag, Tokyo, 1998) p. 72.
15) N. Yagi, Y. Suzuki, K. Umetani, Y. Kohmura and K. Yamasaki: Med. Phys. **26** (1999) 2190.
16) V. E. Cosslett and W. C. Nixon: Nature **168** (1951) 24.
17) V. E. Cosslett and W. C. Nixon: J. Appl. Phys. **24** (1953) 616.
18) M. Born and E. Wolf: *Principles of Optics* (Pergamon Press, Oxford, New York, Toronto, Sydney, Braunschweig, 1975) 5th ed.
19) M. Ando, H. Sugiyama, A. Maksimenko, W. Pattansiriwisawa, K. Hyodo and X. Zhang: Jpn. J. Appl. Phys. **40** (2001) L844.
20) M. Ando, K. Hyodo, H. Sugiyama, A. Maksimenko, W. Pattanasiriwisawa, K. Mori, J. Roberson, E. Rubenstein and Y. Tanaka: Jpn. J. Appl. Phys. **41** (2002) 4742.
21) K. Hirano, A. Maksimenko, H. Sugiyama and M. Ando: Jpn. J. Appl. Phys. **41** (2002) L595.
22) K. Kohra: J. Phys. Soc. Jpn. **17** (1962) 589.
23) M. Ando, Y. Satow, H. Kawata, T. Ishikawa, P. Spieker and S. Suzuki: Nucl. Instrum. & Methods A **264** (1986) 144.
24) K. Umetani, Y. Suzuki and N. Yagi: SPring-8 Information **4** (1999) 50 [in Japanese].
25) S. Goto, K. Takeshita, Y. Suzuki, H. Ohashi, Y. Asano, T. Kimura, N. Matsushita, M. Yagi, H. Isshiki, H. Yamazaki, Y. Yoneda, K. Umetani and T. Ishikawa: Nucl. Instrum. & Methods in Phys. Res. A **467/468** (2001) 682.